Charge-compensation effects and their influence on spectroscopic properties of alkali halides doped with $Cr(CN)_6^{3-}$ ions; the case of a NaBr host

1997 J. Phys.: Condens. Matter 9 1369

(http://iopscience.iop.org/0953-8984/9/6/020)

J. Phys.: Condens. Matter **9** (1997) 1369–1380. Printed in the UK PII: S0953-8984(97)76037-5

Charge-compensation effects and their influence on spectroscopic properties of alkali halides doped with $Cr(CN)_6^{3-}$ ions; the case of a NaBr host

K Hermanowicz

Institute for Low Temperatures and Structure Research, Polish Academy of Science, Wrocław, Poland

Received 8 July 1996, in final form 7 November 1996

Abstract. The Raman scattering, vibrational, electron spin-resonance, electron and luminescence spectra of the $Cr(CN)_6^{3-}$ ion in a sodium bromide crystal host are reported. The results indicate that the complex ion is trapped in two nonequivalent symmetries, which have been identified and characterized by the parameters $\langle g \rangle$, E and D of the spin Hamiltonian and Δ and B of the crystal field. The IR and Raman spectra are discussed on the basis of possible symmetries of the trapped ion. Following vibrational analysis the vibronic assignment of the phosphorescence spectrum is proposed. The role and influence of the charge-compensational configurations as regards the spectroscopic properties of the chromium (III) ion are analysed.

1. Introduction

The understanding of the spectral behaviour of complex-transition-ion impurities in insulating hosts is based upon the concept that the crystal matrix environment modifies spectroscopic properties and the symmetry of the free complex ion [1]. Information concerning the properties of the free complex ion and the nature of the host site into which the ion ($Cr(CN)_6^{3-}$ in this case) is to be incorporated is needed. The identity of the nearest neighbourhood is a very important aspect of the crystal site. The octahedral $Cr(CN)_6^{3-}$ ion replaces the MX_6^{5-} groups in the crystal host during the growth of the doped crystals. Thus, two cation vacancies are created at each Cr^{3+} ion to keep the crystal electrically neutral. The vacancies occupy positions near or next to the complex-ion centre. D_{2h}, D_{4h} and C_s are the most probable symmetries for configurations formed by the complex ion and two vacancies [2]. It is interesting to show how interactions between the doped ion and associated vacancies can modify the properties of the active ion. This paper is a continuation of our earlier studies on the spectroscopy of the hexacyanochromate (III) ion in different alkali halides [3].

2. Experimental details

Single crystals of NaBr doped with potassium chromicyanide were grown by slow evaporation, over P_2O_5, of a saturated aqueous solution of sodium bromide containing 5% of $K_3Cr(CN)_6$ by weight at 50 °C. The concentration of the impurity ion in the crystals obtained was determined in the way described previously [4] and was about 2500 ppm.

0953-8984/97/061369+12$19.50

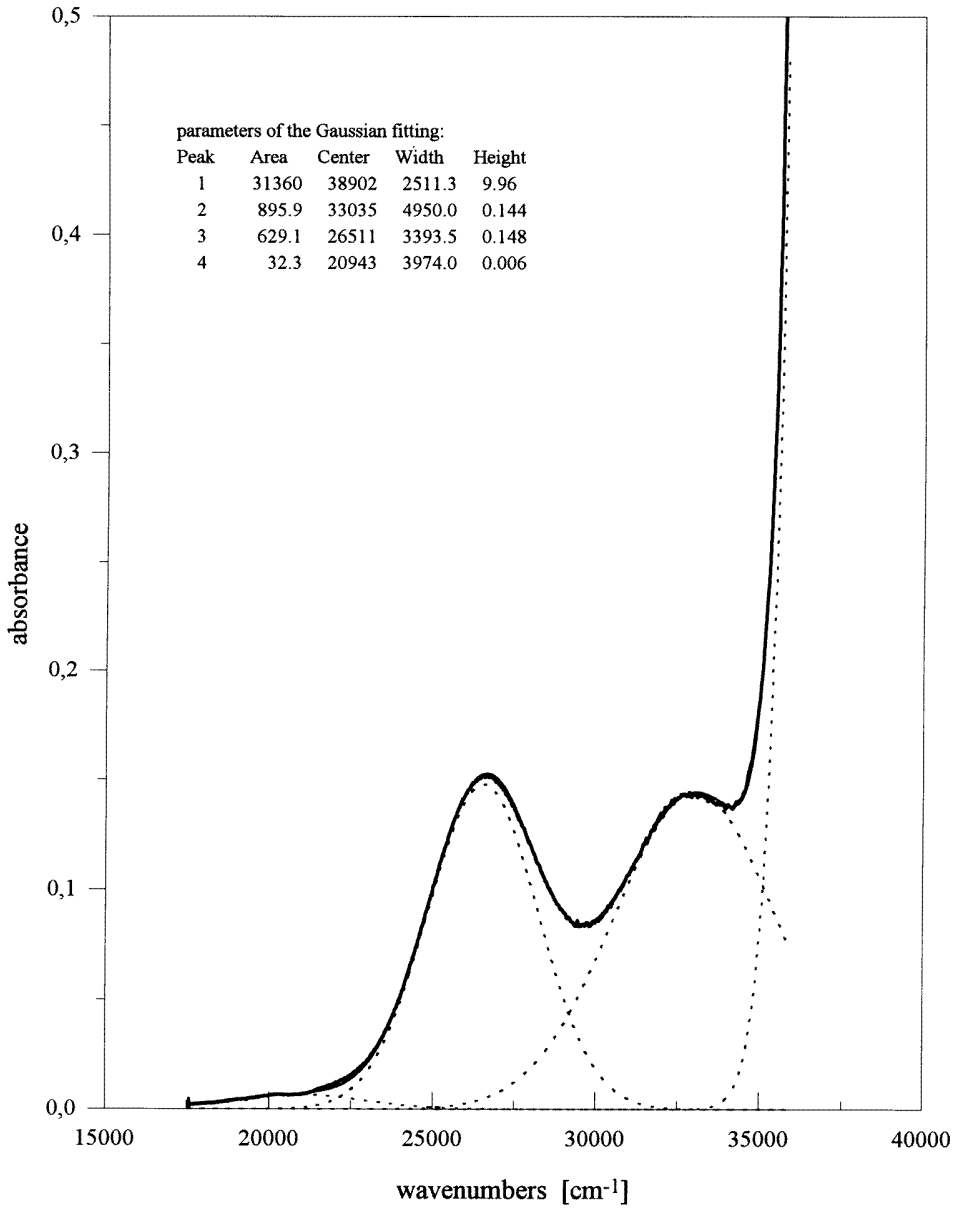

Figure 1. The room temperature electron absorption spectra of $Cr(CN)_6^{3-}$ ions doped into a NaBr host.

Infrared spectra of doped NaBr crystals were recorded at 40 K and room temperature (RT) by means of an M80 Zeiss Jena Spectrophotometer.

The Raman spectra were excited with an argon-ion laser emitting about 150 mW at 4880 Å. Detection was carried out by means of a DFS 24 double-grating monochromator and photon-counting equipment with a cooled GaAs Burle photomultiplier.

Electron absorption spectra were taken with a Varian Model 2300 spectrophotometer.

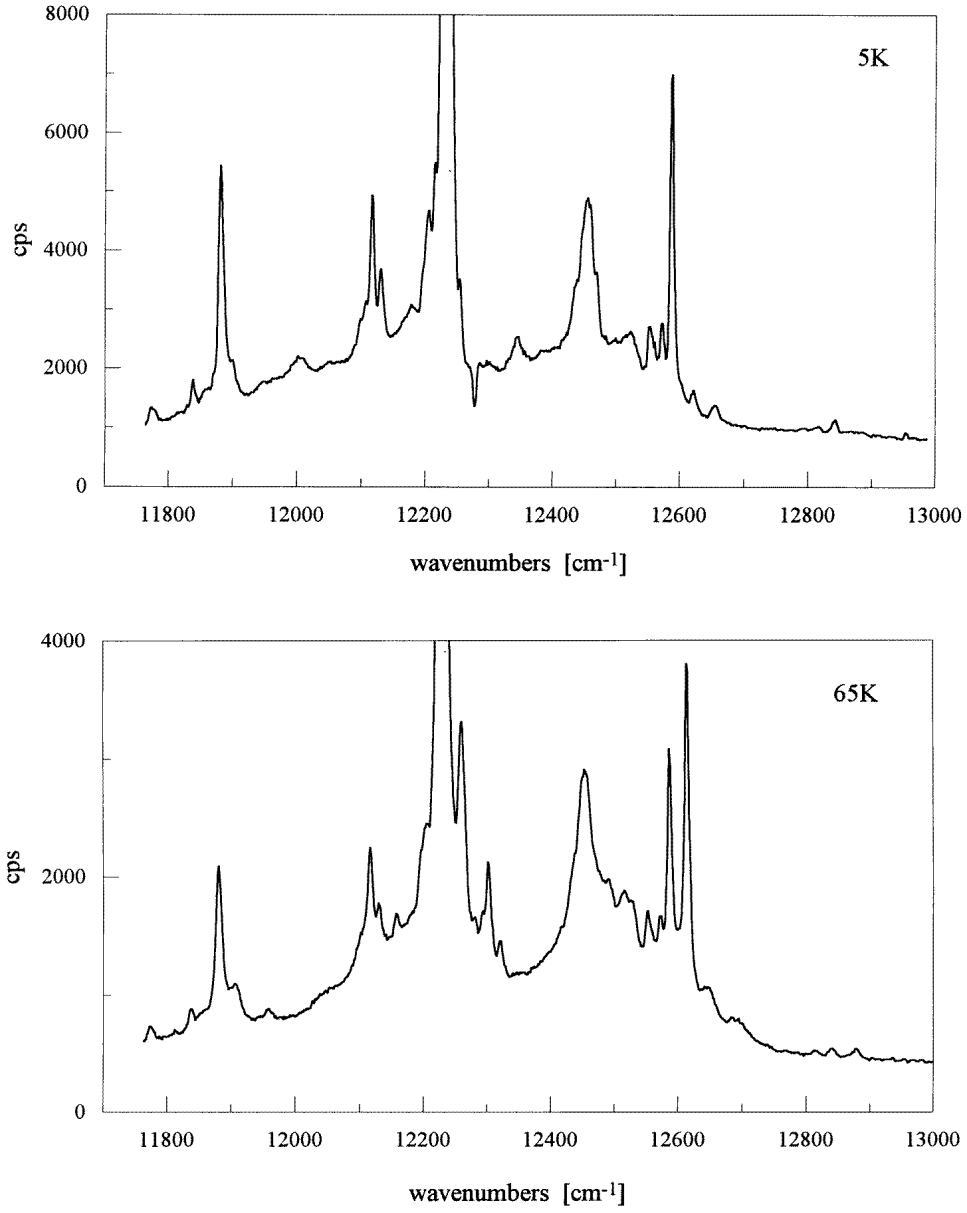

Figure 2. The ^2E_g–$^4A_{2g}$ emission spectra of NaBr:Cr(CN)$_6^{3-}$ crystals at 65 and 5 K.

Emission spectra were recorded from RT down to 5 K using the same instrument and conditions as for the Raman scattering studies.

The ESR spectra of Cr(CN)$_6^{3-}$ in NaBr, with the magnetic field applied along the [100] and the [110] directions, were recorded using an ESR spectrometer manufactured by Wrocław Technical University (Poland).

The low-temperature measurements for the emission studies were made using an Oxford Cryostat Model CF 1204.

Table 1. (a) Assignment of the lines with growing intensity with temperature. $R_2 = 12\,614$ cm^{-1}, L = 34 cm^{-1}. (b) Assignment of the lines with a small temperature dependence. $R_1 = 12\,587$ cm^{-1}, L = 34 cm^{-1}.

(a) Energy (cm^{-1})	Relative intensity*	ΔE (cm^{-1})	Assignment
12 880	w	−293	$R_2 + \nu_8 - L$
12 816	vw	−229	$R_2 + \nu_8 - \nu_{13}$
12 695	vw	−81	$R_2 + \nu_7 - \nu_8$
12 686	vw	−72	$R_2 + \nu_7 - \nu_{12}$
12 646	vw	−32	$R_2 + L$
12 614	s	0	R_2
12 516	w	98	$R_2 - \nu_{13} + L$
12 511	w	103	$R_2 - \nu_7 + \nu_8$
12 498	vw	116	$R_2 - \nu_9 + L$
12 491	w	123	$R_2 - \nu_{13}$
12 484	vw	130	$R_2 - \nu_{13}$
12 478	vw	136	$R_2 - \nu_8 + \nu_9 + L$
12 321	w	293	$R_2 - \nu_8 + L$
12 303	m	311	$R_2 - \nu_8 + L$
12 294	w	320	$R_2 - \nu_8$
12 261	m	353	$R_2 - \nu_8$
12 160	w	454	$R_2 - \nu_7$
11 957	w	657	$R_2 - 2\nu_8$
11 909	w	705	$R_2 - 2\nu_8$
11 813	vw	801	$R_2 - \nu_7 - \nu_8$

3. Results and discussion

3.1. Absorption and emission spectra

The octahedral strong-field ground configuration t_{2g}^3 of Cr^{3+} gives rise to one quartet (^4A_g) and three doublet states (^2E_g, $^2T_{1g}$ and $^2T_{2g}$). The excited configuration $t_{2g}^2 e_g$ gives the states $^4T_{2g}$ and $^4T_{1g}$. Therefore for the crystal studied, three spin-allowed bands corresponding to $^4A_{2g}(F)$–$^4T_{2g}(F)$, $^4A_{2g}(F)$–$^4T_{1g}(F)$ and $^4A_{2g}(F)$–$^4T_{1g}(P)$ transitions should be active. The room temperature absorption spectra of the hexacyanochromate ion trapped in the host studied are shown in figure 1. The spectral contour consists of two strong bands near 33 035 and 26 511 cm^{-1} and a weak shoulder near 20 943 cm^{-1}. The observed strong bands correspond to the first spin-allowed transitions mentioned above, respectively. The trapping of the $Cr(CN)_6^{3-}$ ion in the NaBr host does not discernibly remove the triple degeneracy of the excited states. The observed very weak band at about 20 943 cm^{-1} corresponds to the activated spin-forbidden $^4A_{2g}$–$^2T_{2g}$ transition, because the remaining two doublets lie lower than the $^2T_{2g}$ state for the crystal field with $\Delta/B = 49$ (in this case). The calculated values of the crystal-field parameters Δ and B are 26 511 cm^{-1} and 544 cm^{-1}, respectively.

The zero-phonon $^4T_{2g}$ level lies above the zero-phonon ^2E_g state for the strong ligand field formed by the cyanide groups of the chromium ion. Therefore ^2E_g–$^4A_{2g}$ phosphorescence should be observed for the crystal studied. The emission spectra at 65 and 5 K for the NaBr matrix are shown in figure 2. The ^2E_g energy weakly depends on the strength of the ligand field. The 0–0 band is relatively weak in relation to the vibronic components for the complex ion occupying the site with an inversion symmetry. For the ligands having

Table 1. (Continued)

(b) Energy (cm^{-1})	Relative intensity*	ΔE (cm^{-1})	Assignment
13 123	w	−533	$R_1 + \nu_9 + \nu_8$
12 840	w	−253	$R_1 + 2\nu_{13}$
12 742	vw	−155	$R_1 + \nu_9$
12 655	w	−68	$R_1 + \nu_7 - \nu_{12}$, $R_1 + \nu_7 - \nu_8 - L$
12 621	w	−34	$R_1 + L$
12 587	s	0	R_1
12 572	w	15	$R_1 - \nu_{12} + \nu_8$, $R_1 - L$
12 560	vw	27	$R_1 - \nu_{12} + \nu_8$, $R_1 - \nu_9 + \nu_{13}$
12 552	w	35	$R_1 - L$
12 527	vw	60	$R_1 - \nu_{13} + 2L$, $R_1 - \nu_8 + \nu_9 + \nu_{13}$
12 470	vw	117	$R_1 - \nu_7 + \nu_8$, $R_1 - \nu_9 + L$
12 460	m	127	$R_1 + \nu_{13}$
12 455	s	132	$R_1 - \nu_7 + \nu_8 - L$, $R_1 - \nu_7 + 2\nu_9$
12 449	m	138	$R_1 - \nu_7 + \nu_8 - L$, $R_1 - \nu_7 + 2\nu_9$
12 436	w	151	$R_1 - \nu_9$
12 416	vw	171	$R_1 - \nu_7 + \nu_9 + \nu_{13}$, $R_1 - \nu_8 + \nu_9$
12 280	vw	307	$R_1 - \nu_8 + L$, $R_1 - \nu_9 - \nu_{13} - L$
12 238	s	319	$R_1 - \nu_8 + L$
12 225	vs	362	$R_1 - \nu_8 - L$
12 216	sh	371	$R_1 - \nu_8 - L$, $R_1 - \nu_{12}$
12 207	w	380	$R_1 - \nu_8 - L$, $R_1 - \nu_{12} - L$
12 198	w	389	$R_1 - \nu_8 - L$, $R_1 - \nu_{12} - L$
12 179	vw	408	$R_1 - \nu_7 + L$
12 132	w	455	$R_1 - \nu_7$
12 118	m	469	$R_1 - \nu_7 - L$
12 108	vw	479	$R_1 - \nu_7 - L$
12 098	vw	489	$R_1 - \nu_7 - L$
12 051	vw	536	$R_1 - \nu_{12} - \nu_9$
11 943	vw	644	$R_1 - \nu_8 - 2\nu_9$
11 899	w	688	$R_1 - 2\nu_8$
11 881	m	706	$R_1 - 2\nu_8$
11 861	vw	726	$R_1 - \nu_8 - \nu_{12}$
11 853	vw	734	$R_1 - \nu_8 - \nu_{12}$, $R_1 - 2\nu_8 - L$
11 839	w	748	$R_1 - 2\nu_{12}$
11 781	vw	806	$R_1 - \nu_7 - \nu_8$
11 774	w	813	$R_1 - 2\nu_8 - \nu_{13}$

*s = strong, vs = very strong, m = medium, w = weak, vw = very weak, sh = shoulder.

low-lying π^*-orbitals such as CN^-, the ^2E_g–$^4A_{2g}$ emission is shifted to longer wavelengths due to delocalization of the d electrons [5]. The luminescence spectra of NaBr crystals doped with $Cr(CN)_6^{3-}$ ions are similar to those of KBr and KCl hosts. For the KCl host the positions of the zero-phonon lines R_1 and R_2 of the ^2E_g state were found to follow the low-temperature behaviour. The R_2 line is considerably stronger for higher temperatures. The Arrhenius plot of its temperature dependence for KCl crystal shows an activation energy close to the result of subtracting the energy of the R_2 line from that of the next predominant line, which was assigned to the R_1 transition. A similar doublet of lines, assigned as the 0–0 transition, is observed for the NaBr host at 12 587 and 12 614 cm^{-1}.

Three intense vibronic patterns can be distinguished in the emission spectrum near the 0–0 lines appearing at 98–171, 290–389 and 408–489 cm^{-1}. They correspond to the odd-

parity internal modes: $\nu_9(F_{1u}) = 156$ cm^{-1} and $\nu_{13}(F_{2u}) = 126$ cm^{-1}; $\nu_8(F_{1u}) = 339$ cm^{-1}; and $\nu_7(F_{1u}) = 459$ cm^{-1}, which are connected with δ(CCrC), δ(CrCN) and δ(CrC) metal–ligand vibrations and their combinations with lattice phonons, respectively. The vibronic modes in the 500–800 cm^{-1} range are due to the overtones and combinations of the internal vibrations. Hence their intensities are an order of magnitude smaller than those in the remaining regions. The weak lines observed at 15–35 cm^{-1} are probably due to librational or translational lattice vibrations of the trapped ion. It should be pointed out that the most intense vibronic pattern corresponds to the ν_8-mode, whose energy is close to the activation energy $\varepsilon = 300$ cm^{-1} evaluated by Stręk and Trabjerg [6] on the basis of the temperature dependence of the phosphorescence decay. The vibronic assignments of the bands observed for the luminescence spectra of the crystal studied are proposed in table 1.

3.2. Infrared and Raman scattering spectra

The IR and RS spectra of the NaBr:$Cr(CN)_6^{3-}$ crystal are shown in figure 3. The assignment of the observed bands to the respective vibrational modes is made on the basis of infrared and Raman scattering studies of $K_3Cr(CN)_6$ single crystal [7, 8] and is presented in table 2.

Table 2. Vibrational frequencies (cm^{-1}) of the $Cr(CN)_6^{3-}$ ion in a NaBr host.

Vibration	Type	Activity	IR*	RS
				2131
ν_1	C≡N stretching	A_{1g}(R)		2130
				2128
ν_3	C≡N stretching	E_g(R)		2126
				2124
ν_6	C≡N stretching	F_{1u}(IR)	2135vw	
			2130vw	
			2125m	
			2121m	
ν_7	Cr≡C stretching	F_{1u}(IR)	454s	
			449s	
				405
ν_{10}	Cr–CN bending	F_{2g}(R)		395
				387
ν_{12}	Cr–CN bending	F_{2u}(inactive)		
ν_2	Cr–C stretching	A_{1g}(R)		352
			354s	
ν_8	Cr–CN bending	F_{1u}(IR)	343s	
			331s	
ν_4	Cr–C stretching	E_g(R)		337
				296
ν_5	C–Cr–C bending	F_{1g}(inactive)		278
				258

*s = strong, vs = very strong, m = medium, w = weak, vw = very weak, sh = shoulder.

The IR spectrum exhibits characteristic groups of the vibrational bands corresponding to the $Cr(CN)_6^{3-}$ ion trapped in the alkali halide hosts [3]. In the $\nu_6(F_{1u})$ frequency region a multiplet composed of two strong bands at 2121 and 2125 cm^{-1}, and two very weak shoulders at 2130 and 2135 cm^{-1} are observed. They correspond to the stretching vibrations of the CN group. The number of multiplet components is smaller than for earlier-studied hosts. Another vibrational pattern composed of bands at 331, 343 and 354 cm^{-1} should be

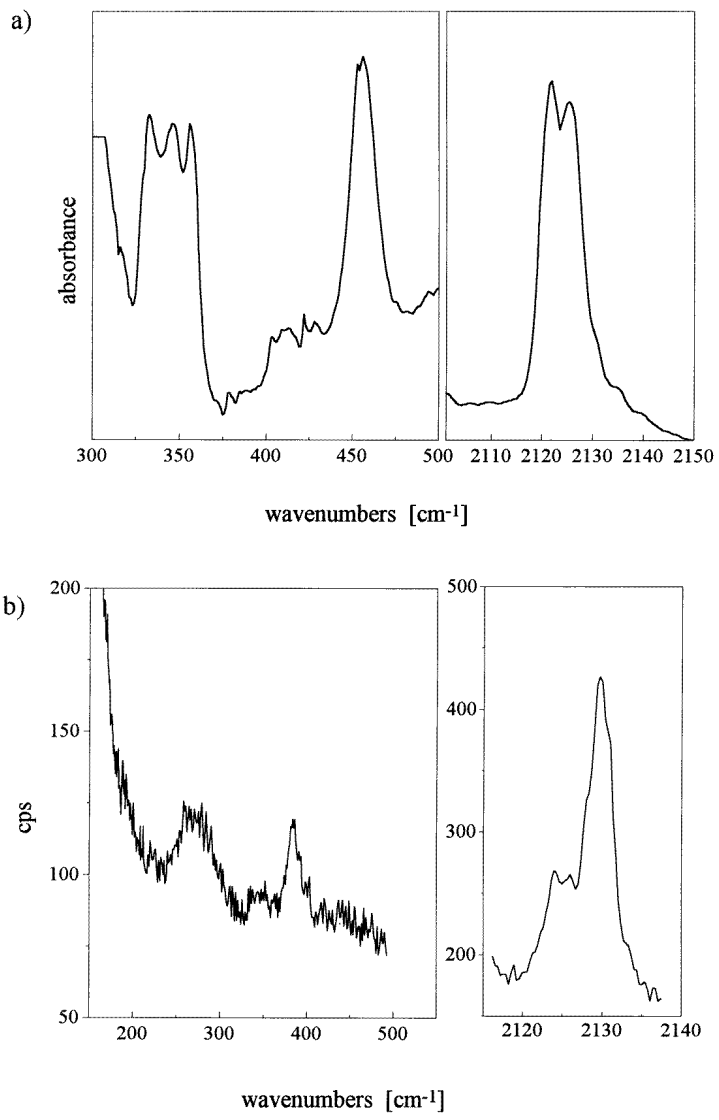

Figure 3. The room temperature IR (a) and RS (b) spectra observed in the 200–500 and 2100–2150 cm^{-1} ranges for the Cr(CN)$_6^{3-}$ ion in a NaBr host.

assigned to the bending δ(CCrC) mode. The F_{1u} degeneracy of this mode is removed due to the lowering of the complex-ion symmetry from O_h to D_{2h} and C_s in accordance with the results published previously for other host systems. This is indicative of the interactions between the trapped complex ion and two compensation vacancies. The activation of the doublet contour at 449 and 454 cm^{-1} instead of single line in the ν(Cr–C) stretching region also is a result of the charge-compensational interactions of the lattice.

Similar effects are observed for the Raman scattering spectra. The multiplet of five bands in the 2124–2131 cm^{-1} region corresponds to the $\nu_1(A_{1g})$ and $\nu_3(E_g)$ stretching ν(C–N) modes. The $\nu_{10}(F_{2g})$ bending δ(CCrC) modes are observed as a triplet at 387, 395

and 405 cm^{-1} and also the bands activated at 258, 278 and 296 cm^{-1} are assigned to the $\nu_5(F_{2g})$ mode, inactive for the O_h symmetry of the complex ion. All of the spectra contain considerably more components than is predicted theoretically for an octahedral active ion trapped in a cubic host. The number of multiplet components for the ν_6-modes connected with cyanide groups is larger than those for the ν(CrC) and δ(CCrC) bands, which may suggest that the influence of the compensation gaps on the central ion is much higher in the outer sphere than in the CrC_6 polyhedron.

3.3. Electron paramagnetic resonance spectra

Electron paramagnetic resonance measurements were used in this work due to the sensitivity of this method to the environment and the influence of the nearby defects on the spectral symmetry of the doped ion. This advantage allows one to determine the symmetry of the configuration centres formed by the $Cr(CN)_6^{3-}$ ion and two vacancies. The spectra recorded are very complicated and contain numerous lines. They can be interpreted in terms of the Hamiltonian [9]: $H = \beta \boldsymbol{H} g \cdot \boldsymbol{S} + D[S_z^2 - (1/3)S(S+1)] + E(S_x^2 - S_y^2) + A\boldsymbol{S} \cdot \boldsymbol{J}$, where β is the Bohr magneton, $\boldsymbol{H}$ is the applied magnetic field, g is the spectroscopic splitting factor, the effective spin $\boldsymbol{S}$ is 3/2 for three unpaired electrons, D represents the effect of an initial splitting due to axial-symmetry fields, E is the departure from this axial symmetry and the last term represents the interaction between the electron and the magnetic moment of the nucleus with the nuclear spin $\boldsymbol{J}$. The hyperfine interaction was not observed due to the low abundance of the chromium nuclei with nuclear spin 3/2.

The parameters of the fine structure were determined by studying the angular dependence of the EPR signals. The measurements revealed the equivalence of the $\boldsymbol{y}$- and $\boldsymbol{z}$-axes of the crystal-field gradient of the Cr(III) ion. The analysis of the EPR signal anisotropy allowed us to distinguish, like for the alkali halides studied earlier, two main groups of lines corresponding to the two predominant types of differently oriented centres of D_{2h} and C_s symmetry. A detailed analysis of this problem was described by Wang *et al* [10].

The present centres could be characterized by spin-Hamiltonian parameters obtained from [100] and [110] measurements (figure 4). The zero-field splitting parameters $\langle g \rangle$, D and E were evaluated from a fitting procedure [11] which was based upon the simulation of the angular dependence of the resonance field as the parameters $\langle g \rangle$, D and E were varied. The parameters evaluated for the centres identified are given in table 3.

Table 3. The parameters evaluated for the centres identified. The g-parameter values are found to be nearly isotropic and are 1.991 ± 0.001.

	Parameters			
Centre	g	D (cm^{-1})	E (cm^{-1})	$a = E/D$
D_{2h}	1.991	0.0982	0.034	0.33
C_s	1.991	0.0805	0.024	0.30

From the relation between the fine-structure parameter D and the crystalline field around the doped paramagnetic ion [12]: $D = k(\lambda/\Delta)^2 V$ (λ: spin–orbit coupling coefficient; k: constant; V: trigonal-field parameter; Δ: cubic-field parameter), the assumption may be made that the axiality parameter D, characterizing the distortion of the $Cr(CN)_6^{3-}$ octahedron in the host, should be proportional to $1/R^3$, where R is the effective distance between the central ion and the gaps, i.e. the cationic vacancies, which takes different values for centres

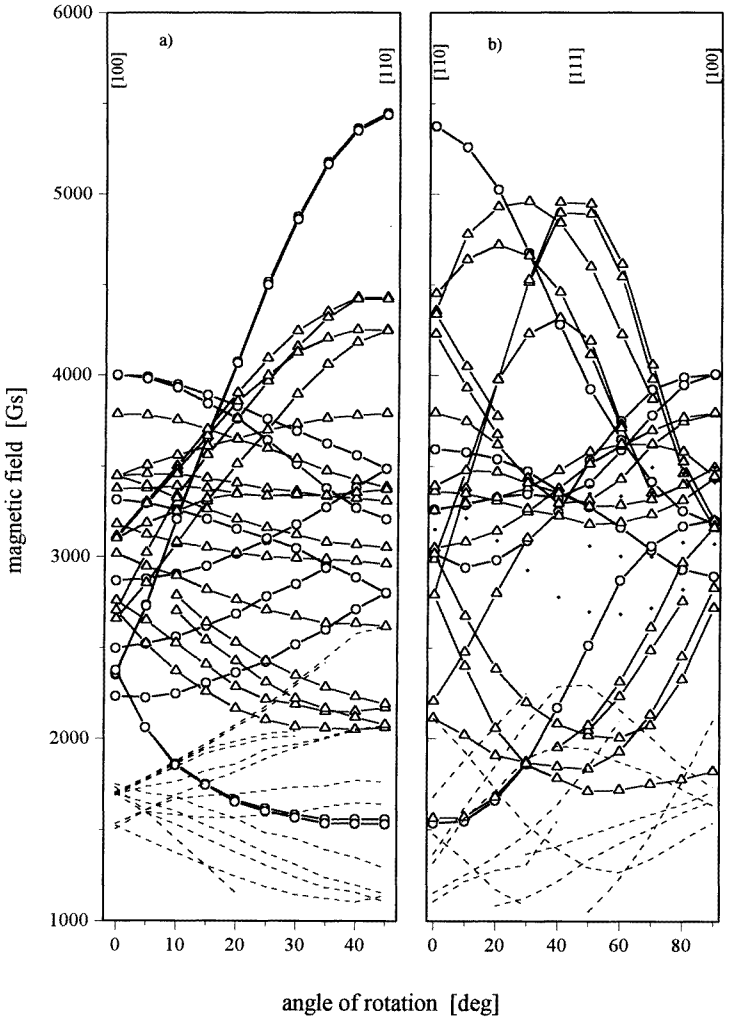

Figure 4. The angular dependencies of the fine structure of the Cr(CN)$_6^{3-}$ ion in the (100) (a) and (110) (b) planes. The solid lines represent allowed ($\Delta M_s = \pm 1$) transitions of D_{2h} (lines with open circles) and C_s (lines with upright triangles) centres. The forbidden transitions ($\Delta M_s = \pm 2, \pm 3$) are also shown by the dotted lines.

I and II. The relation between R_{I} for centre I and R_{II} for centre II is $R_{\mathrm{II}} \cong 1.08 R_{\mathrm{I}}$, i.e. it remains the same as for other alkali halide hosts. The evaluated values of the fine-structure parameters for the hexacyanochromate ion incorporated in a sodium bromide host are close to those observed for the KCl host and represent the extremely rare distortion case with $E/D = 1/3$.

4. Conclusions

(a) The comparison of some spectroscopic parameters such as Δ, D, ν_6 and the unit-cell parameter of the host can give more detailed information concerning the nature and

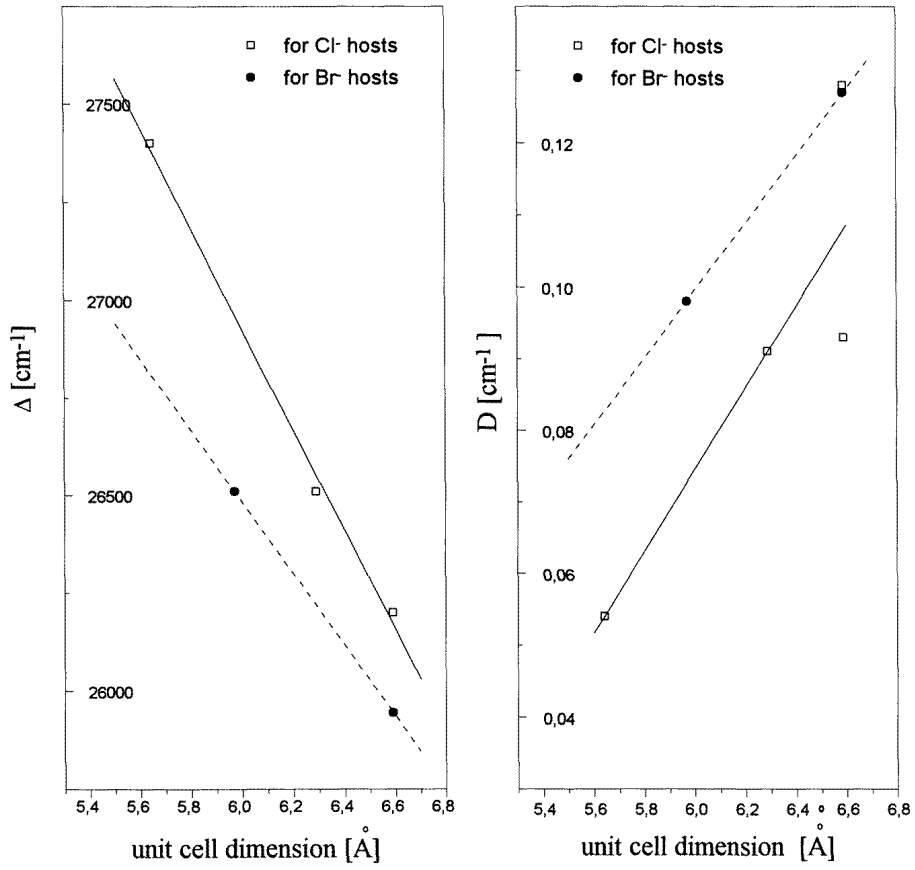

Figure 5. Plots of the crystal-field, Δ, and fine-structure, D, parameters, and the frequencies, ν_6, of the C≡N stretching modes versus the host lattice dimension (a) for the $Cr(CN)_6^{3-}$ ion in the alkali halides studied: NaCl ($a = 5.64$ Å); NaBr ($a = 5.97$ Å); KCl ($a = 6.29$ Å); KBr and RbCl ($a = 6.59$ Å).

the strength of the matrix crystal field. The dependencies of the crystal-field (Δ) and fine-structure (D) parameters, and the frequency ν_6 on the lattice dimension are shown in figure 5.

In the halide series the observed parameters change almost linearly with the lattice dimension. For the chloride hosts the crystal-field strength of the outer halide sphere acting on the complex ion rises more strongly than for the bromide analogue. This fact is in accordance with the strength of the field for the halide ligand in the spectrochemical series. It should be pointed out that only two bromide hosts were available; however, some attributes of the matrix field acting on the trapped ion are clearly pronounced.

(b) A lowering of the site symmetry from octahedral occurs for the $Cr(CN)_6^{3-}$ ion in a NaBr host. It is manifested by a splitting of the bands observed in IR and RS spectra due to the removal of the degeneracy of some vibrations, the raising of the oscillator strengths of the electronic transitions, and the appearance of the ^2E_g phosphorescence for the chromium (III) ion.

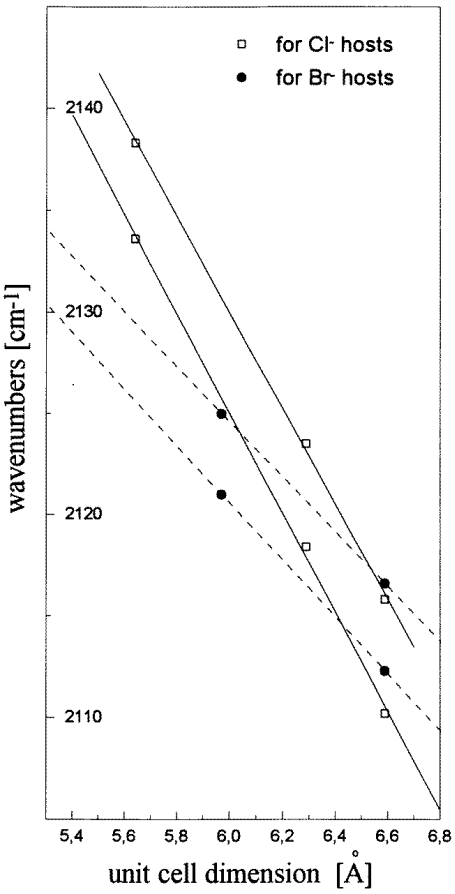

Figure 5. (Continued)

(c) Among the possible configurations formed by the doped ion and two negatively charged vacancies, the present EPR studies of the hexacyanochromate (III) ion in NaBr demonstrate that the D_{2h} and C_s site symmetries are presented. The D_{2h} centre represents the extremely rare case with E/D very close to 1/3.

(d) The odd-parity modes, F_{1u} and F_{2u}, give the dominant contribution to the promotion of the radiationless transitions of the ^2E_g state (table 1). The relative intensities of the vibronic bands observed in the low-frequency region indicate that the ν_8, δ(M–C=N) deformation mode is the most efficient within this phenomenon.

References

[1] Narayama M, Sivasankhar V S and Radhakrishna S 1981 *Phys. Status Solidi* b **105** 11
[2] Jain S C, Warrier A V R and Seghal K H 1972 *J. Phys. C: Solid State Phys.* **5** 1511
Jain S C, Warrier A V R and Seghal K H 1973 *J. Phys. C: Solid State Phys.* **6** 193
[3] Hanuza J, Hermanowicz K, Jeżowska-Trzebiatowska B and Waplak S 1989 *J. Mol. Struct.* **212** 255
[4] Hanuza J, Stręk W, Hermanowicz K, Jeżowska-Trzebiatowska B and Trabjerg I 1986 *J. Mol. Struct.* **144** 141
[5] Chatterjee K K and Forster L S 1964 *Spectrochim. Acta* **20** 1603

[6] Stręk W and Trabjerg I 1986 *Physica* C **141** 323
[7] Hanuza J and Jeżowska-Trzebiatowska B 1975 *Acta Phys. Polon.* A **47** 155
[8] Jensen P W 1973 *J. Mol. Struct.* **17** 377
[9] Abragam A and Bleaney B 1970 *Electron Paramagnetic Resonance of Transition Ions* (Oxford: Clarendon) p 430
[10] Wang D M, Hutton D R and Pilbrow J R 1986 *J. Phys. C: Solid State Phys.* **19** 789
[11] O'Reilly D E and Schacher G E 1965 *J. Chem. Phys.* **43** 4222
[12] Meyer P H and Gerristen H J 1955 *Phys. Rev.* **100** 742